

# Time–Temperature Dependence of the Electrical Resistivity of High-Density Polyethylene/Carbon Black Composites

Matteo Traina, Alessandro Pegoretti, Amabile Penati

Department of Materials Engineering and Industrial Technologies (DIMTI) and Italian Interuniversity Consortium on Materials Science and Technology (INSTM) Research Unit, University of Trento, Via Mesiano 77, 38050 Trento, Italy

Received 8 January 2007; accepted 11 March 2007

DOI 10.1002/app.26444

Published online 23 July 2007 in Wiley InterScience (www.interscience.wiley.com).

**ABSTRACT:** Several carbon blacks with surface areas from 105 to 1353 m<sup>2</sup>/g were used to produce composites through melt compounding with a high-density polyethylene matrix. The electrical behavior of the obtained composites was investigated by the measurement of their resistivity as a function of the carbon black content and type at various temperatures and times during isothermal annealing treatments. The percolation threshold markedly decreased as the carbon black surface area increased, reaching a minimum value of 1.8 vol % for the carbon black with a surface area of 1353 m<sup>2</sup>/g. The resistivity

passed through a maximum as the test temperature increased. Moreover, the analysis of the experimental data evidenced that the host high-density polyethylene matrix and the conductive carbon black network rearranged during the isothermal thermal treatments, causing a resistivity decrease. This rearrangement became less and less important as the carbon black surface area increased. © 2007 Wiley Periodicals, Inc. *J Appl Polym Sci* 106: 2065–2074, 2007

**Key words:** nanocomposites; polyethylene (PE); annealing

## INTRODUCTION

Polymers are generally insulating materials from an electrical point of view. One way of improving their conductivity is the addition of conductive fillers such as metal powders or fibers, graphite, carbon black (CB), and carbon fibers.<sup>1–4</sup> The electrical behavior of these systems has been successfully described by the percolation theory.<sup>5–7</sup> After a given critical content, the so-called percolation threshold, the conductive particles form a conductive network that extends through the whole system. In the percolation region, the resistivity drastically decreases by several orders of magnitude.

In the case of the CB-filled composites, the behavior is strongly dependent on the CB microstructure.<sup>3,8–11</sup> CB is generally formed by small primary particles fused together in aggregates. Moreover, these aggregates can be agglomerated into more extended structures. Depending on the compounding process, the agglomerates can be destroyed during mixing in a polymeric matrix, but the aggregates remain unchanged. The dimensions of the primary

particles can be estimated by the measurement of the specific surface area (SSA). In particular, the SSA increases as the diameter of the primary particles decreases. On the other hand, the structure of the aggregates, which is a measure of the three-dimensional fusion of CB particles, is traditionally evaluated by the measurement of the oil adsorption number (OAN). OAN increases as the structure complexity, that is, the size/shape distribution, of the aggregates increases. As a general rule, the percolation threshold decreases as SSA or OAN increases because of the formation of a more efficient conductive network.

The electrical behavior of these materials is markedly influenced by the temperature. For the conductive composites based on crystalline polymers, the resistivity increases as the temperature increases. In fact, for these materials, a positive temperature coefficient (PTC) effect has been reported.<sup>8,10–26</sup> This phenomenon is generally ascribed to differences in the coefficient of thermal expansion between the host matrix and the filler particles. In particular, the higher thermal expansion of the polymer matrix partially destroys the continuity of the conductive network, thus causing an increase in the volume resistivity. At temperatures higher than the melting point of the polymer matrix, the resistivity decreases as the temperature increases. This trend is generally called a negative temperature coefficient (NTC) effect.<sup>8,10–13,16–19,21–24,26–28</sup> This phenomenon is related

Correspondence to: A. Pegoretti (alessandro.pegoretti@ing.unitn.it).

Contract grant sponsor: Eurostandard S.p.A. (Trento, Italy).

**TABLE I**  
**Properties of the CBs Used as Fillers for the HDPE–CB Composites**

Material code	Grade	Supplier	Density (g/cm <sup>3</sup> )	OAN (cm <sup>3</sup> /g)	SSA (m <sup>2</sup> /g)
CB1	Raven P-FE/B	Columbian Carbon Europa SRL (Via San Cassiano 140, 28069 San Martino Di Trecate, Italy)	1.92	0.98	105
CB2	Conductex 975u	Columbian Carbon Europa SRL (see above)	1.94	1.69	226
CB3	Vulcan XC72	Cabot Italiana SPA (Zona Industriale, 4; 38055 Grigno, Italy)	1.93	1.78	231
CB4	Ketjenblack EC300J	Akzo Nobel Chemicals SPA (Via Eliseo Vismara 80; 20020 Arese, Italy)	1.92	3.22	802
CB5	Ketjenblack EC600JD	Akzo Nobel Chemicals SPA (see above)	1.95	4.95	1353

to the increased mobility of the filler particles in the molten polymer, which can rearrange themselves into a more efficient conductive network.<sup>21,24,29</sup> From a more general point of view, the microstructure of the polymer matrix and the conductive network depends on both the temperature and time. In fact, in analogy to various mechanical and thermal properties, the resistivity of a conductive polymer composite may change with time during an isothermal annealing treatment.<sup>10,11,13,16,21,25,26,30</sup>

This work deals with the electrical behavior of high-density polyethylene (HDPE) and CB composites. The time–temperature dependence of the resistivity of these composites was analyzed as a function of the filler content and CB microstructure for composites produced with various CBs and different filler contents. In particular, the resistivity was evaluated under three different testing conditions: (1) at room temperature, (2) as a function of temperature at a constant heating rate, and (3) as a function of time during isothermal annealing treatments.

## EXPERIMENTAL

### Materials

The polymeric matrix was an Eltex A4009 HDPE kindly supplied by BP Solvay (Solvay SA: Rue du Prince Albert 44, 1050 Bruxelles, Belgium), now Innovene, in the form of a fine powder. This HDPE had a melt flow rate of 0.8 g/10 min (evaluated at 190°C and 2.16 kg) and a density of 0.958 g/cm<sup>3</sup> at 23°C.

Five different types of CBs were used, whose characteristic properties, such as the density determined by X-ray diffraction measurements, the SSA determined by the Brunauer–Emmett–Teller method (ASTM D 6556-03), and the OAN determined with *n*-dibutyl phthalate (ASTM D 2414-04), are summarized in Table I.

### Resistivity measurements of the CBs

The measurement of the electrical volume resistivity of the CBs was realized at room temperature in a direct-current mode with a voltage of 1 V and with

a Metex ME-32 digital multimeter. A sample of approximately 1 g of CB was compressed in a hollow Teflon cylinder with an inner diameter of 21 mm between two metal plungers at compression pressures ranging from 10 to 250 kPa. These pressures were obtained by the placement of calibrated metallic masses on the top plunger. The resistivity was hence determined as a function of the degree of compressive packing, that is, the apparent specific volume, of the CB. This latter quantity was evaluated by the continuous measurement of the volume variation of the compressed CB mass by a digital comparator.

### Composite preparation

The dried HDPE and CB powders were mixed and then melt-compounded with a Thermo-Haake Poly-lab Rheomex PTW 16p corotating, intermeshing twin-screw extruder with a screw diameter of 16 mm, a length-to-diameter ratio of 25, and a sheet die. Barrel temperatures were set at 130, 200, 210, 220, and 220°C, and a screw speed of 12 rpm was used for all the composites. The extruder produced a continuous sheet with a cross section of 50 × 1.5 mm<sup>2</sup> that was collected on a special conveyor belt. The maximum investigated CB content was about 18 vol %.

### Resistivity measurements of the HDPE–CB composites

The measurement of the electrical volume resistivity of HDPE–CB composites in a direct current was performed under two different testing configurations. For materials with a resistivity higher than 10<sup>7</sup> Ω cm, the resistivity through the plane was determined with a Keithley 6517A electrometer under an applied voltage of 1000 V. Specimens in the form of square plaques with a side of 40 mm were punch-cut and placed between two disk electrodes. A conductive paint was applied to the surface in contact with the electrodes to reduce the contact resistance. For the specimens having a resistivity lower than 10<sup>7</sup> Ω cm, the resistivity in the extrusion direction was determined by the application of a voltage of 1 V and

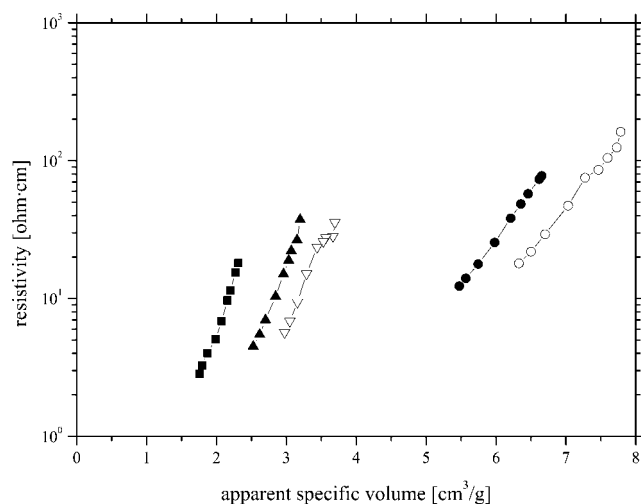


**Figure 1** Resistivity as a function of the apparent specific volume for the various CBs: (■) CB1, (▲) CB2, (▽) CB3, (●) CB4, and (○) CB5.

with a Metex ME-32 digital multimeter. The samples were in the form of strips ( $100 \times 5 \times 1.5 \text{ mm}^3$ ), and conductive paint was applied on the ends to which the electrodes were attached.

The temperature dependence of the resistivity was also analyzed for composites with resistivity values lower than  $10^7 \text{ } \Omega \text{ cm}$ . The measurements were made in a thermostatic chamber that allowed the resistivity as a function of temperature to be measured from room temperature up to  $200^\circ\text{C}$  at a constant heating rate of  $1^\circ\text{C}/\text{min}$ . For the same composites, the effects of an isothermal annealing treatment were also investigated. The samples were placed in a thermostatic chamber at a constant temperature ( $60$ ,  $90$ , or  $120^\circ\text{C}$ ) for  $24 \text{ h}$ , and their resistivity was measured before and after the treatment and during the treatment as a function of time.

### Differential scanning calorimetry (DSC)

DSC measurements were performed with a Mettler DSC 30 calorimeter. A first heating ramp from  $0$  up to  $200^\circ\text{C}$  was followed by a cooling stage from  $200$  to  $0^\circ\text{C}$  and by a second heating ramp up to  $200^\circ\text{C}$ . Both the heating and cooling rates were fixed at  $10^\circ\text{C}/\text{min}$ , and all tests were conducted in nitrogen flushing at  $100 \text{ mL}/\text{min}$ . The crystallinity content was assessed by the integration of the normalized area of the melting endothermic peak and division of the heat involved by the reference value of a  $100\%$  crystalline linear polyethylene, that is,  $277.1 \text{ J}/\text{g}$ .<sup>31</sup>

## RESULTS AND DISCUSSION

### Resistivity measurements of the CBs

The electrical resistivity of CBs strongly depends on the compaction degree of the aggregates.<sup>3,32–34</sup> In

fact, under compressive loads, CB aggregates tend to rearrange into a more densely packed form, and more contacts between aggregates are created. Figure 1 presents the room-temperature resistivity of the CBs as a function of their apparent specific volume. This figure clearly shows that the resistivity decreases as the packing level increases. This behavior is more and more evident as the SSA and OAN of the CBs increases. As previously reported by Probst and Grivei,<sup>34</sup> the electrical resistivity is expected to decrease with increasing structure. This phenomenon is generally related to a reduction in the contact resistance as the aggregates become more tightly packed and pressed against one another. On a logarithmic scale, all the investigated CBs show a linear dependence on the apparent specific volume. A linear extrapolation to low apparent specific volumes (corresponding to high packing values) allows one to estimate resistivity values in the range of  $10^{-1}$  to  $10^{-2} \text{ } \Omega \text{ cm}$  for all the CBs. In fact, at very low contact resistance, the conductivity mechanism would tend to be governed by the CB graphitic structure, even if the value of  $10^{-2} \text{ } \Omega \text{ cm}$  is still higher than the value of  $10^{-5} \text{ } \Omega \text{ cm}$  typically reported for graphite.<sup>35</sup>

### Room-temperature resistivity of the HDPE–CB composites

Figure 2 shows the room-temperature resistivity of the HDPE–CB composites as a function of the CB content. For all the composites, a trend following the percolation theory can be observed. Above a certain filler content, the resistivity shows a drastic drop from the value of the HDPE matrix, that is approximately  $10^{18} \text{ } \Omega \text{ cm}$  down to a common limiting value of about  $5 \text{ } \Omega \text{ cm}$ . According to the Kirkpatrick

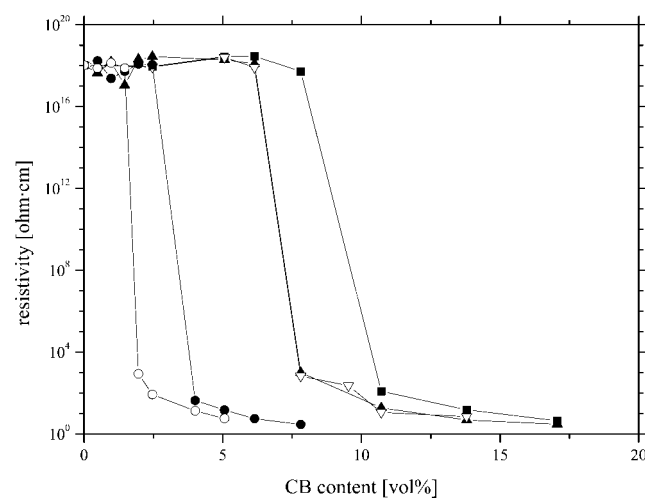


**Figure 2** Room-temperature resistivity of HDPE–CB composites as a function of the CB volume content: (■) HDPE–CB1, (▲) HDPE–CB2, (▽) HDPE–CB3, (●) HDPE–CB4, and (○) HDPE–CB5.

**TABLE II**  
Parameters of the Kirkpatrick Model [Eq. (1)] Obtained from the Best Fitting of the Electrical Resistivity at Room Temperature as a Function of the CB Content

Material code	$\phi_C$ (vol %)	$\rho_0$ ( $\Omega$ cm)	$t$
HDPE-CB1	9.8	0.097	1.85
HDPE-CB2	7.7	0.094	1.81
HDPE-CB3	7.6	0.122	1.90
HDPE-CB4	3.1	0.036	1.83
HDPE-CB5	1.8	0.045	1.78

model,<sup>36</sup> which applies to insulating (polymeric matrix)–conductor (conductive filler) systems, the composite resistivity ( $\rho$ ) at filler contents above the percolation threshold ( $\phi_C$ ), can be fitted by a power-law equation in the following form:

$$\rho = \rho_0(\phi - \phi_C)^{-t} \quad (1)$$

where  $\rho_0$  is a reference resistivity depending on the filler,  $\phi$  is the filler volume fraction, and  $t$  is an exponential factor. The best fitting of the experimental data of Figure 2 with eq. (1) allows one to assess the parameters reported in Table II for all the HDPE–CB composites. For all the composites, a similar reference resistivity value (i.e., ca.  $10^{-1}$   $\Omega$  cm) can be observed, which is consistent with the values of CB resistivity. Moreover, the exponential factor is in the range of 1.5–2, which is typical for systems in which the filler reaches a homogeneous dispersion.<sup>6,36</sup> The percolation threshold of the CB-filled composites markedly depends on the CB structure. In particular, the percolation threshold decreases as the SSA and OAN parameters increase. The following Janzen equation<sup>9</sup> has been proposed to correlate the percolation threshold to the OAN value of the CB:

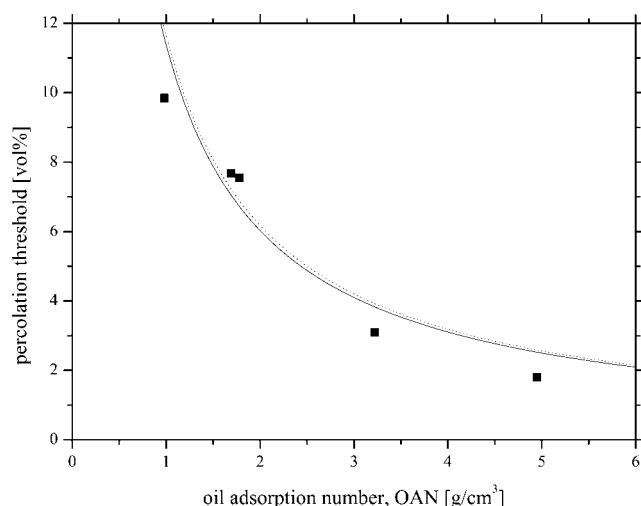


**Figure 3** Percolation threshold as a function of OAN of (■) CB. The lines represent Janzen's equation [eq. (2)] for  $d = 1.90$   $\text{g}/\text{cm}^3$  (solid line) and for  $d = 1.95$   $\text{g}/\text{cm}^3$  (dotted line).

$$\phi_C = \frac{1}{1 + 4 \cdot d \cdot \text{OAN}} \quad (2)$$

where  $d$  is the CB density. As evidenced in Figure 3, the experimental data are in quite good agreement with the provisions of eq. (2).

### Temperature dependence of the resistivity of the HDPE–CB composites

Figure 4 describes the trend of the resistivity as a function of the temperature typically observed for the HDPE–CB composites investigated in this study. In particular, Figure 4(a,b) presents data obtained for the HDPE–CB2 and HDPE–CB5 composites, respec-

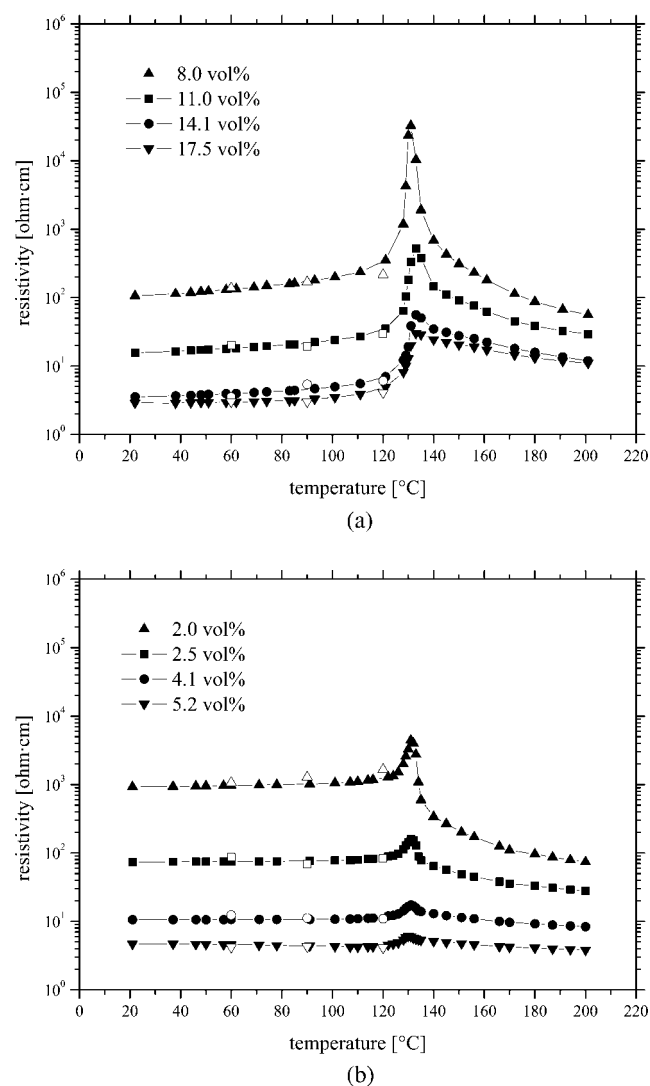


**Figure 4** Temperature dependence of the resistivity values for (a) HDPE–CB2 and (b) HDPE–CB5 composites filled with various CB amounts. The open symbols refer to the resistivity of the same materials at the end of an isothermal annealing of 24 h at the indicated temperatures.

tively, that is, composites realized with CBs having relatively low and relatively high SSAs. In these plots, the resistivity shows a clear peak located at 132–134°C. It is therefore possible to distinguish two regions: a first region at temperatures before the maximum in which the resistivity follows a PTC trend and a second one after the maximum in which the resistivity shows an NTC trend. Typically, the PTC effect has an onset temperature at 120–122°C; after that, the increasing of the resistivity becomes very sharp. Similarly, the NTC effect is characterized by an endpoint temperature of about 143–145°C, after which the decreasing of the resistivity levels off. This behavior has been observed for all the conductive HDPE–CB composites here investigated, the characteristic temperatures being independent of the filler content or type. As previously proposed for several polymer/CB composites,<sup>10–15,17,22–24,26,27</sup> the resistivity–temperature behavior can be directly correlated to the melting temperature of the polymeric matrix. In fact, DSC analysis carried out on the HDPE matrix shows the onset of the melting at 124°C, the melting peak at 135°C, and the endpoint at 147°C; the crystallinity was about 80%. These values are not substantially affected by the CB presence: at high filler amounts, the CB induces only a slight decrease in the crystallinity (<5%). The values of the onset, peak, and endpoint of the melting transition are the same as those observed on the resistivity–temperature curves. The magnitude of the PTC and NTC effects strongly depends on the CB amount and type. In particular, PTC and NTC effects become more and more pronounced as the CB content decreases, and for a given CB content, the SSA and OAN values decrease. This behavior is in good agreement with the existing literature.<sup>10,11,13,14,17–19,37,38</sup> PTC and NTC effects can be analyzed in different ways. A simple approach refers to a parameter called the PTC intensity,<sup>10,11,13,15,17</sup> which is defined as the ratio of the maximum observed resistivity to the corresponding room-temperature value. Similarly, the NTC intensity is usually defined as the ratio of the maximum resistivity value to the resistivity observed in the molten state (200°C in our case). These parameters are reported in Figure 5 as a function of the CB content of the HDPE–CB composites. According to the existing literature,<sup>10,11,13,15,17</sup> as the filler content increases, the intensities of the PTC and NTC parameters decrease. Moreover, as the surface area of the CB increases, the intensities of the PTC and NTC effects markedly decrease. This behavior could be ascribed to a more efficient conductive network obtained in highly structured composites produced with increasing filler content and surface area.

Another possible approach to analyzing these data is based on the fitting of the resistivity–temperature

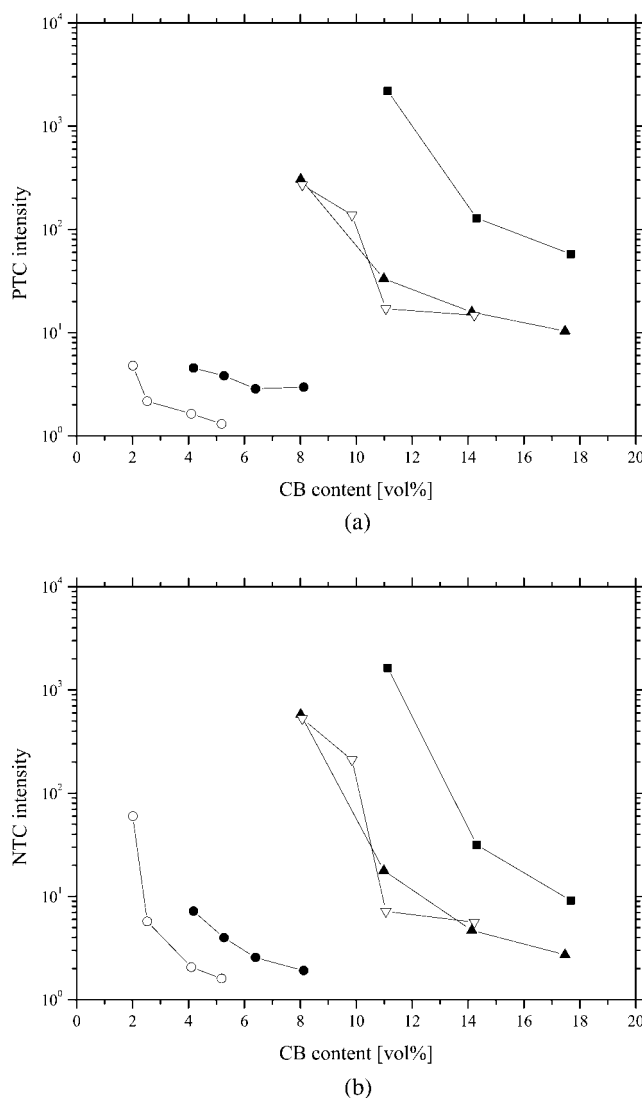


**Figure 5** (a) PTC and (b) NTC intensities as functions of the CB content for various HDPE–CB composites. See Figure 2 for an explanation of the symbols.

curves. In the existing literature, an exponential equation [eq. (3)]<sup>37</sup> and a power-law equation [eq. (4)]<sup>13</sup> have been proposed:

$$\rho = \rho_0 + \Delta\rho \cdot \exp(-m/T) \quad (3)$$

$$\rho = \rho_0 + \Delta\rho \cdot T^m \quad (4)$$

where  $\rho_0$ ,  $\Delta\rho$ , and  $m$  are parameters derived from the fitting of the experimental data. In both cases,  $m$  is the most relevant parameter for describing the PTC and NTC effects because it directly correlates with the slope of the resistivity–temperature curve. As a general rule, the PTC and NTC effects become more and more important as parameter  $m$  increases. To improve its accuracy, the fitting procedure is con-

**TABLE III**  
**Parameter  $m/1000$  of the Exponential Law [Eq. (3)] and Parameter  $m$  of the Power Law [Eq. (4)] from the Best Fitting of the Experimental Data in Various Regions of the Resistivity–Temperature Curves**

Material code	$\phi$ (vol %)	$m$ for PTC-1	$m/1000$ (K)			
			PTC-1	PTC-2	NTC-1	NTC-2
HDPE–CB1	11.1	17.1	6.4	229.8	–130.7	–13.8
	14.3	14.2	5.4	111.4	–84.5	–10.5
	17.7	14.1	5.4	41.3	–58.3	–8.4
HDPE–CB2	8.0	11.1	4.3	116.8	–240.7	–10.9
	11.0	10.3	3.9	30.8	–88.6	–9.1
	14.1	11.1	4.3	11.5	–60.6	–4.7
HDPE–CB3	17.5	18.1	6.8	5.2	–48.1	–4.9
	8.1	12.3	3.9	86.9	–109.1	–6.4
	9.8	14.1	4.6	58.2	–95.4	–2.8
HDPE–CB4	11.1	11.9	3.9	15.1	–32.6	–1.7
	14.2	14.0	4.4	10.6	–38.0	–2.4
	4.2	15.0	5.7	37.7	–31.1	–6.3
HDPE–CB5	5.3	16.3	6.2	19.6	–18.4	–3.3
	6.4	18.3	6.9	12.2	–17.2	–4.5
	8.1	20.5	7.7	1.8	–12.9	–3.8
HDPE–CB5	2.0	16.0	5.7	126.8	–43.0	–11.0
	2.5	25.7	8.9	41.4	–17.8	–6.9
	4.1	36.8	14.4	10.1	–10.3	–5.1
	5.2	0.8	1.7	3.2	–5.9	–4.9

ducted separately on four different regions of the resistivity–temperature curves. The first low-temperature region is related to a mild PTC effect (PTC-1), the second one is related to a sharp PTC effect (PTC-2), the third one is related to a sharp NTC effect (NTC-1), and the last one is related to a mild NTC effect (NTC-2). The results of the fittings, that is, the  $m$  parameter as a function of the CB contents for the various HDPE–CB composites in the four different temperature regions, are presented in Table III. The power-law equation can reasonably fit the experimental results only in the PTC-1 region, the fitting in the other regions being very poor. As a result, only the results of the fitting in the PTC-1 region are reported for the power-law equation. In general, the data obtained from the fitting with both eqs. (3) and (4) partly confirm the considerations previously reported for the PTC and NTC intensities. In fact, in the PTC-2, NTC-1, and NTC-2 regions, the absolute value of parameter  $m$  shows a tendency to decrease as the filler content increases, but a clear correlation with the CB surface area is not evident. Moreover, the absolute value of parameter  $m$  increases to very high values in all the HDPE–CB composites when the filler content approaches the percolation threshold. A peculiar case is the one regarding the PTC-1 region. Only for the highly structured HDPE–CB composites does  $m$  show a tendency to increase as the filler content increases. At present, we do not have a clear explanation for this behavior, which is in contrast to that reported by Foulger<sup>13</sup> on the same subject.

#### Resistivity during the isothermal annealing of the HDPE–CB composites

Figure 6 reports the typical trend of the resistivity as a function of time during an isothermal annealing treatment. During the initial minutes of the treatment, the resistivity increases from the room-temperature value up to a maximum according to an inverse exponential law. This step takes about 1–5 min and can be attributed to heat transmission phenomena in the sample. After an equilibrium temperature is reached, the resistivity decreases with an exponential trend, asymptotically approaching a constant value after approximately 300 min. In the remaining time up to completion of the test (24 h), the resistivity further decreases no more than 5%. This behavior is in agreement with previous works.<sup>10,11,25,26</sup> According to Zhang et al.,<sup>26</sup> this phenomenon can be fitted by an exponential equation of the following form:

$$\rho = \rho_0 + \Delta\rho \cdot \exp\left(-\frac{t}{\tau}\right) \quad (5)$$

where  $\rho_0 + \Delta\rho$  represents the initial maximum resistivity value,  $\rho_0$  is a limiting resistivity constant value, and  $\tau$  is a characteristic decay time. To analyze the effects of the selected annealing treatments on the electrical resistivity of the composites, a relative resistivity reduction at room temperature and at the treatment temperature has been defined as the percentage reduction of the resistivity before and after the treatment. Figure 7 shows the relative resistivity

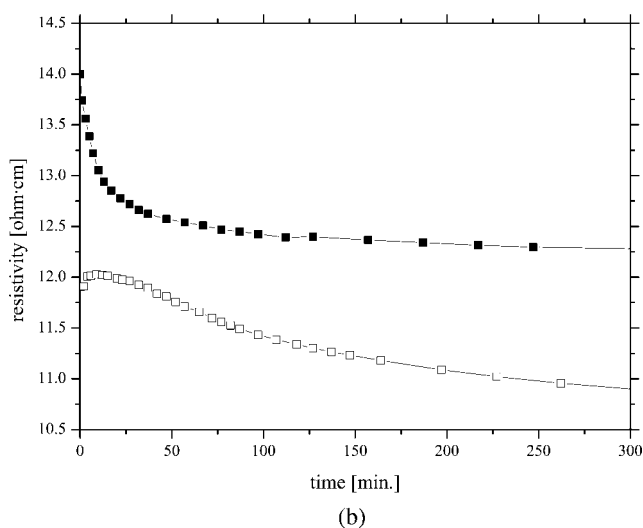
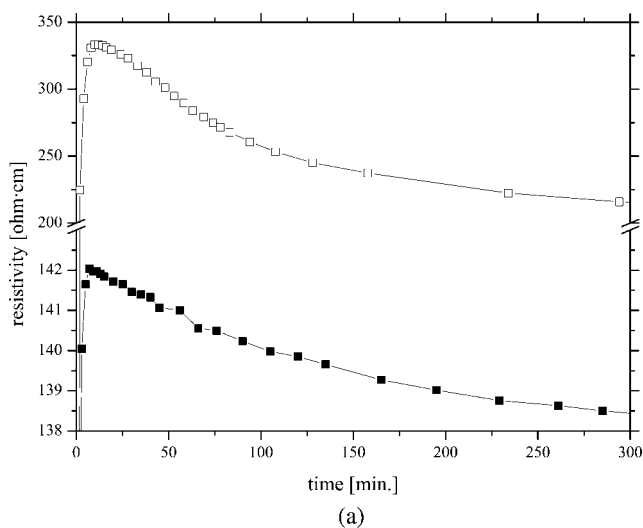


**Figure 6** Resistivity as a function of time during the isothermal annealing treatment: (a) HDPE filled with 8.1 vol % CB2 tested at (■) 60 and (□) 120°C and (b) HDPE filled with 4.1 vol % CB5 tested at (■) 60 and (□) 120°C.

reduction at the treatment temperature as a function of the CB content for the HDPE–CB composites at various treatment temperatures. At the lower annealing temperature, that is, 60°C, the resistivity reduction does not show a particular trend as a function of the CB content and type. At higher temperatures, such as 90 and 120°C, the relative resistivity reduction decreases as the CB content increases. The CB type does not seem to play a major role. In the case of the treatment at 90°C, the values reaches a maximum of about 20%, which rises up to 40% at 120°C, a temperature close to the melting of the polymeric matrix. The same results (data not reported) have been obtained for the relative resistivity at room temperature.

The decay time does not show any clear dependence on the isothermal annealing treatment temperature, the CB type, or the CB content. Zhang et al.<sup>26</sup>

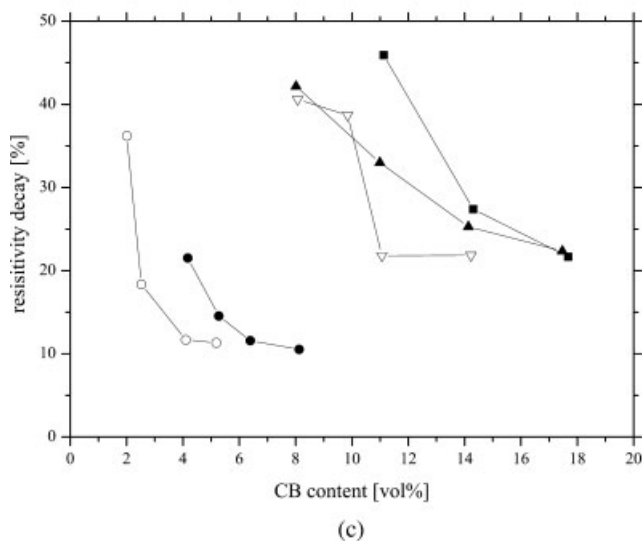
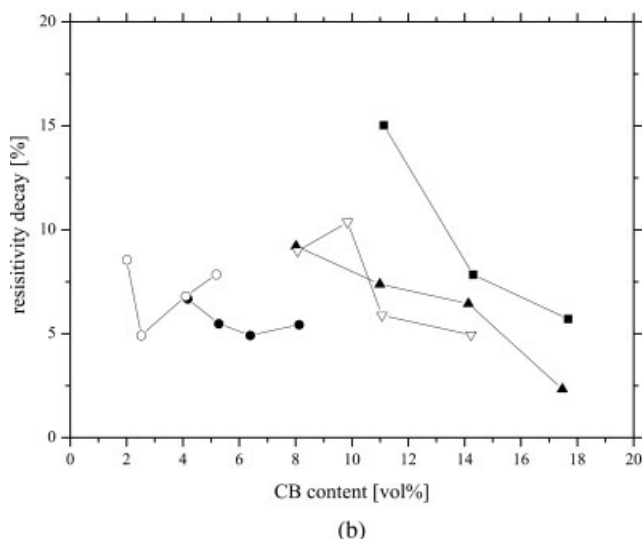
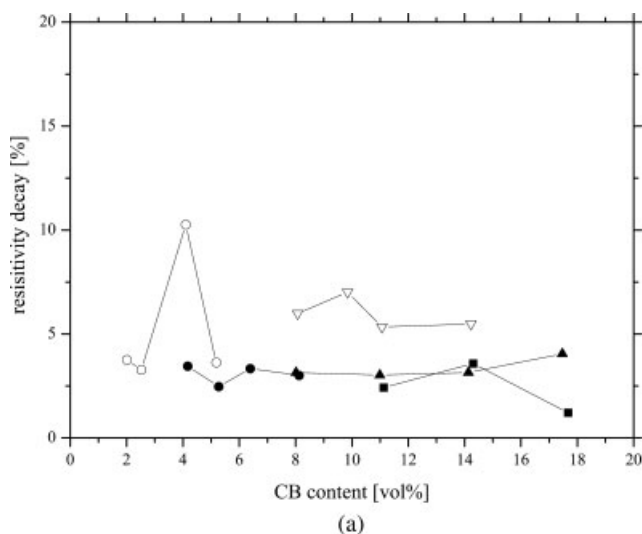


**Figure 7** Relative resistivity reduction at the treatment temperatures of (a) 60, (b) 90, and (c) 120°C as a function of the CB content for various HDPE–CB composites. See Figure 2 for an explanation of the symbols.

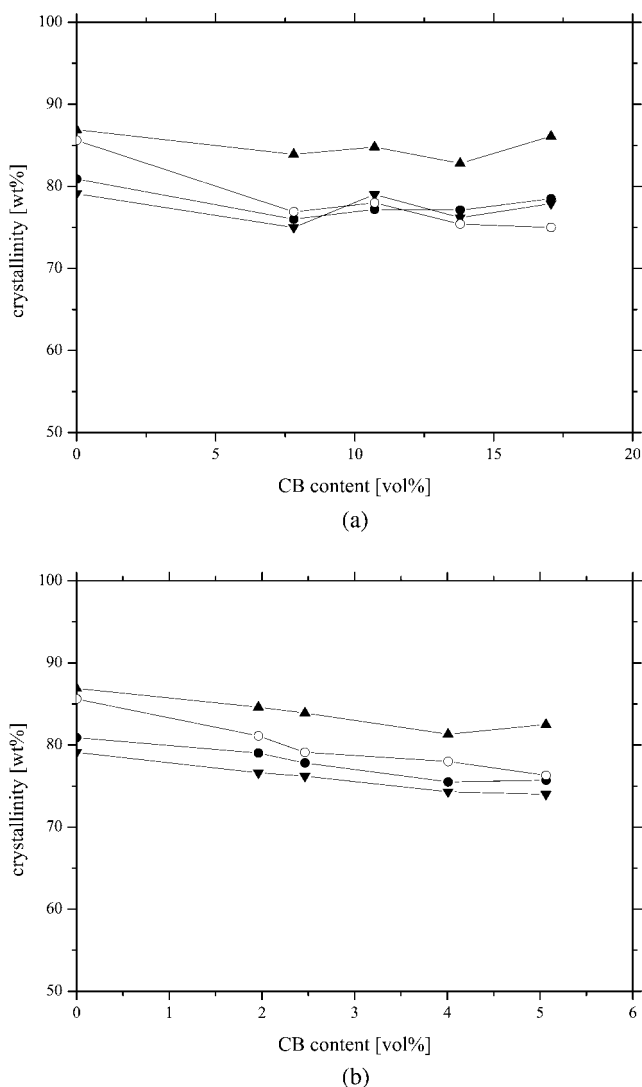


**Figure 8** Crystallinity of the (a) HDPE-CB2 and (b) HDPE-CB5 composites ( $\blacktriangledown$ ) before an isothermal annealing treatment and after an isothermal annealing treatment for 24 h at the treatment temperatures of ( $\bullet$ ) 60, ( $\circ$ ) 90, and ( $\blacktriangle$ ) 120°C.

found a decrease in the decay time as the treatment temperature increased.

Moreover, there is a good agreement between the resistivity values measured after 24 h during the isothermal annealing treatment and the resistivity values measured as a function of the temperature with respect to the treatment temperature for all the materials (see the open points in Fig. 4). From these data, it follows that the observed resistivity-temperature data are equilibrium data: the heating rate is low enough to allow a dynamic rearrangement of the conductive filler network.

To evaluate the effect of the isothermal annealing treatment, DSC analysis was carried out on the materials before and after the isothermal annealing treatment. The analyzed materials were the HDPE-CB2 composites, the HDPE-CB5 composites, and the

HDPE matrix: the latter underwent the isothermal annealing treatments as a reference even if the resistivity-time dependence was too low to be measured. The crystallinity levels, as assessed with the DSC analysis, are presented in Figure 8. These data show that the isothermal annealing treatment at 120°C improved the crystallinity of all the materials by 5–8%. Although this phenomenon was observed also for the HDPE matrix treated at 60 and 90°C, it was more limited in the case of the HDPE-CB5 composites and completely absent in the case of the HDPE-CB2 composites.

### Time-temperature dependence of the resistivity of the HDPE-CB composites

Figure 9 permits us to visualize the effects of the temperature and time on the resistivity of the HDPE-CB composites. In this figure, the resistivity as a function of the CB content is reported (1) at room temperature, (2) at room temperature after an isothermal annealing treatment, and (3) at the peak of the resistivity-temperature curves. As a general rule, the isothermal annealing treatment induces a decrease in the resistivity, whereas resistivity values at the peaks of the resistivity-temperature curves evidence an increase. Both these phenomena are more and more intense as the SSA of the CB decreases. In all cases, the resistivity curves not only vertically translate but also change their shape. In fact, the PTC intensity (Fig. 5), which is directly related to the peak of the resistivity-temperature curves, and the resistivity reduction at room temperature induced by the isothermal annealing treatment

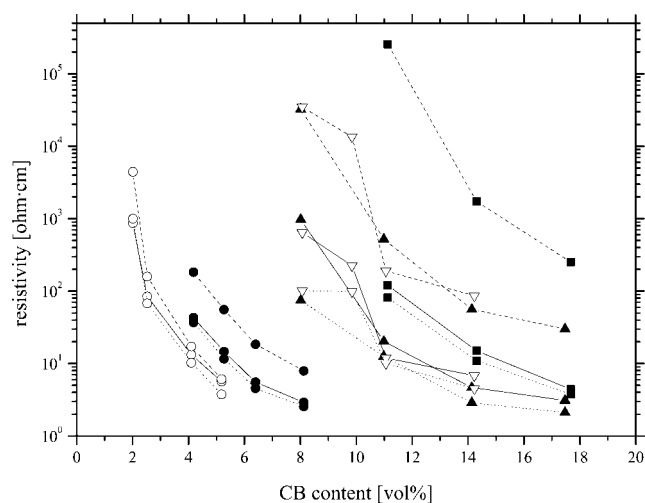


**Figure 9** Resistivity of the HDPE-CB composites as a function of the CB content under different conditions: (—) at room temperature, ( $\cdots$ ) at room temperature after an isothermal annealing treatment at 120°C, and (---) at the peak for the resistivity-temperature curve. See Figure 2 for an explanation of the symbols.



**TABLE IV**  
**Parameters of the Kirkpatrick Model [Eq. (1)] Obtained from the Best Fitting of the Electrical Resistivity as a Function of the CB Content**

Material code		$\phi_C$ (vol %)	$\rho_0$ ( $\Omega$ cm)	$t$
HDPE-CB1	IA	8.8	0.034	2.38
	P	10.2	0.160	3.40
HDPE-CB2	IA	6.4	0.058	2.04
	P	7.4	0.224	2.65
HDPE-CB3	IA	6.6	0.078	2.06
	P	7.5	0.392	2.60
HDPE-CB4	IA	3.0	0.028	1.86
	P	3.4	0.098	1.82
HDPE-CB5	IA	1.9	0.031	1.79
	P	1.9	0.038	1.88

The resistivity was considered at room temperature after an isothermal annealing treatment at 120°C (IA) and at peak values during temperature variation (P).

(Fig. 7), which is directly related to the resistivity at room temperature after the isothermal annealing treatment, evidence a clear dependence on the CB content.

According to the Kirkpatrick model, the data of Figure 7 can be fitted with a power-law equation [eq. (1)], whose best fitting parameters are summarized in Tables II and IV. In comparison with the as-produced HDPE-CB composites evaluated at room temperature, the percolation threshold and reference resistivity increase for the systems evaluated at the resistivity-temperature peak, whereas they decrease after the isothermal annealing treatment. Exponential factor  $t$  increases in both cases, but the increase is more enhanced in the case of the resistivity evaluated at the resistivity-temperature peak. This behavior is more and more evident for HDPE-CB composites filled with lower surface area CB, whereas for the composites filled with higher surface area CB, it is negligible.

The results of this analysis imply that the rearrangements occurring as effects of the temperature and time are not governed by linear viscoelasticity. The change in the parameters is complex and depends on the initial microstructure of the composites and on the thermal treatment. The effect of the thermal treatment on the microstructure of the conductive filler network can be evidenced with parameter  $t$ . In the literature, the values of the exponential factor are in the range of 1.5–2 for systems in which the filler has an homogeneous dispersion,<sup>6,36</sup> the values greater than 2 generally being correlated to a nonhomogeneous dispersion of the filler in the polymeric matrix.<sup>39–42</sup> In this way, it is possible correlate the change of  $t$  to a change of the microstructure. Hence, the temperature induces rearrangements of the conductive filler network in the host matrix that leads to a segregation phenomenon. In fact, several authors have observed a preferential segregation of

the CB in the amorphous regions.<sup>13,14,29,43</sup> DSC analysis confirms that the resistivity reduction becomes more and more important when the crystallinity improvement becomes markedly evident. The rearrangements of the filler appear to be more and more evident as the surface area of the CB decreases. This behavior could be explained by the consideration that a highly structured CB restrains the local mobility of the polymer chain and thus the possibility of intensive rearrangements.

## CONCLUSIONS

In this work, the electrical behavior of HDPE-CB composites was investigated, with particular attention given to the time-temperature dependence of the resistivity. In agreement with the literature data, our results evidence that the percolation threshold decreases as the CB surface area increases and that the intensities of PTC and NTC effects decrease as the CB content and surface area increase, especially at temperatures near the melting region. The isothermal annealing treatments evidence that the resistivity decreases as a function of time, following an exponential law: the resistivity reduction produced by an isothermal annealing is more pronounced as the filler content increases and the temperature approaches the melting point.

From a general point of view, the thermal treatments, both at a constant heating rate and isothermal, induce filler rearrangements in the host polymer matrix. The analysis of exponential factor  $t$  and the percolation threshold indicates a possible segregation of the CB thus forming a more efficient conductive filler network. These effects become more and more important as the CB surface area decreases, whereas for composites filled with high surface area CB, the effect is limited.

## References

1. Metal-Filled Polymers: Properties and Applications; Bhattacharya, S. K., Ed.; Marcel Dekker: New York, 1986.
2. Delmonte, J. Metal/Polymer Composites; Van Nostrand Reinhold: New York, 1990.
3. Carbon Black: Science and Technology; Donnet, J. B.; Bansal, R. C.; Wang, M. J., Eds.; Marcel Dekker: New York, 1993.
4. Wypych, G. Handbook of Fillers; ChemTec: New York, 2000.
5. Lux, F. J Mater Sci 1993, 28, 285.
6. Stauffer, D.; Aharony, A. Introduction to Percolation Theory; Taylor & Francis: New York, 1991.
7. Zallen, R. The Physics of Amorphous Solids; Wiley: New York, 1983.
8. Huang, J. C. Adv Polym Technol 2002, 21, 299.
9. Janzen, J. J Appl Phys 1975, 46, 966.
10. Traina, M.; Pegoretti, A.; Penati, A. Presented at the 1st International Symposium on Nanostructured and Functional Polymer-Based Materials and Composites, Dresden, Germany, 2005.

11. Traina, M.; Pegoretti, A.; Penati, A. Presented at the 27th National Convention of the Italian Association of the Science and Technology of Macromolecules, Naples, Italy, 2005.
12. Bin, Y.; Xu, C.; Zhu, D.; Matsuo, M. *Carbon* 2002, 40, 195.
13. Foulger, S. H. *J Appl Polym Sci* 1999, 72, 1573.
14. Hindermann-Bischoff, M.; Ehrburger-Dolle, F. *Carbon* 2001, 39, 375.
15. Hou, Y. H.; Zhang, M. Q.; Rong, M. Z. *Polym Int* 2004, 53, 944.
16. Hou, Y. H.; Zhang, M. Q.; Rong, M. Z.; Yu, G.; Zeng, H. M. *J Appl Polym Sci* 2002, 84, 2768.
17. Huang, S. J.; Lee, J. K.; Ha, C. S. *Colloid Polym Sci* 2004, 282, 575.
18. Mather, P. J.; Thomas, K. M. *J Mater Sci* 1997, 32, 1711.
19. Mather, P. J.; Thomas, K. M. *J Mater Sci* 1997, 32, 401.
20. Omastová, M.; Proke, J.; Podhradská, S.; Chodák, I. *Macromol Symp* 2001, 170, 231.
21. Park, J. S.; Kang, P. H.; Nho, Y. C.; Suh, D. H. *J Appl Polym Sci* 2003, 89, 2316.
22. Tang, H.; Chen, X.; Luo, Y. *Eur Polym J* 1996, 32, 963.
23. Tang, H.; Chen, X.; Luo, Y. *Eur Polym J* 1997, 33, 1383.
24. Tang, H.; Liu, Z. Y.; Piao, J. H.; Chen, X. F.; Lou, Y. X.; Li, S. H. *J Appl Polym Sci* 1994, 51, 1159.
25. Zhang, C.; Wang, P.; Ma, C. A.; Wu, G.; Sumita, M. *Polymer* 2006, 47, 466.
26. Zhang, J. F.; Zheng, Q.; Yang, Y. Q.; Yi, X. S. *J Appl Polym Sci* 2002, 83, 3112.
27. Song, Y.; Zheng, Q. *Compos Sci Technol* 2006, 66, 906.
28. Vilčáková, J.; Sába, P.; Quadrat, O. *Eur Polym J* 2002, 38, 2343.
29. Lee, M. G.; Nho, Y. C. *Radiat Phys Chem* 2001, 61, 75.
30. Sun, Y.; Luo, S.; Watkins, K.; Wong, C. P. *Polym Degrad Stab* 2004, 86, 209.
31. Brandrup, J.; Immergut, E. H. *Polymer Handbook*; Wiley: New York, 1989; Vol. 9.
32. Celzard, A.; Maréché, J. F.; Payot, F. *J Phys D* 2000, 33, 1556.
33. Celzard, A.; Mareché, J. F.; Payot, F.; Furdin, G. *Carbon* 2002, 40, 2801.
34. Probst, N.; Grivei, E. *Carbon* 2002, 40, 201.
35. Kelly, B. T. *Physics of Graphite*; Applied Science: London, 1981.
36. Kirkpatrick, S. *Rev Mod Phys* 1973, 45, 574.
37. Alexander, M. G. *Mater Res Bull* 1999, 34, 603.
38. Zois, H.; Apekis, L.; Omastová, M. *Macromol Symp* 2001, 170, 249.
39. Mamunya, Y. P.; Davydenko, V. V.; Zois, H.; Apekis, L.; Snarskii, A. A.; Slipchenko, K. V. *Polym Polym Compos* 2002, 10, 219.
40. Mamunya, Y. P.; Muzychenko, Y. V.; Pissis, P.; Lebedev, E. V.; Shut, M. I. *Polym Eng Sci* 2002, 42, 90.
41. Zois, H.; Apekis, L.; Mamunya, Y. P. *Macromol Symp* 2003, 198, 461.
42. Zois, H.; Apekis, L.; Mamunya, M.; Omastová, Y. P. *J Appl Polym Sci* 2003, 88, 3013.
43. Yi, X. S.; Zhang, J. F.; Zheng, Q.; Pan, Y. *J Appl Polym Sci* 2000, 77, 494.